THE AMERICAN SOCIETY OF MECHANICAL ENGINEERS
345 E. 47 St., New York, N.Y. 10017

82-GT-82

An Experimental Investigation of Rotating Stall Flow in a Centrifugal Compressor

N. Kämmer
Research Assistant

M. Rautenberg
Professor
Chief of Department for Radial Compressors

Institute for Turbomachinery and Gasdynamics,
University of Hannover,
Hannover, West Germany

The flow through a centrifugal compressor impeller and a vaneless diffuser was investigated using unsteady pressure transducers and stationary probes when the compressor operated in the rotating stall region of the compressor map. The inlet velocity profile of the impeller was measured with traversing probes and was found to be significantly different from the profiles measured in an unthrottled condition. A zone of reverse flow was detected close to the suction duct wall as well as a strong swirl induced by the impeller. Circumferentially and meridionally spaced transducers made it possible to determine the stall frequency and the number of stall cells. The amplitude of the flow distortion as a function of meridional position was calculated from meridionally spaced transducers.

NOMENCLATURE

a_c = velocity of sound in inlet chamber ,m/s
b = diffuser width, m
c = absolute velocity, m/s
d = diameter, m
f = frequency, Hz
k = constant
m = number of stall cells
$\dot{m}$ = mass flow rate at reference conditions 1.01325 bar and 288.15 K, kg/s
n = compressor speed, rpm
M_u = circumferential Mach number, u_2/a_c
r = radius, m
s = blade length along shroud line, m
T = stagnation temperature, K
u = circumferential velocity, m/s
x = length, m
ß = angle between relative and circumferential velocity, deg
Δ = difference
η = isentropic efficiency, %
λ = diameter ratio d/d_2
π = pressure ratio
φ = angle, rad

Subscripts

a shroud = outer
bl blade
c suction chamber
i hub = inner
g geometrical
tot total-to-total
u circumferential
z axial
1 impeller entry plane
2 impeller exit plane
3 diffuser exit plane

Superscripts

$\bar{}$ = mean value

INTRODUCTION

The reduction of mass flow rate through a centrifugal compressor at constant speed moves the operating point to the left of the compressor map until a limit line is encountered. This limit is frequently referred to as the stall line (1)+ since further reduction of mass flow will cause the compressor to stall and a severely distorted and

+ Numbers in parentheses designate references at end of paper.

Contributed by the Gas Turbine Division of the ASME.

unsteady flow field appears in the compressor. Frequently an operating point cannot be found at all to the left of this stall limit line. It depends on a compression system stability criterion, which one of these two modes of instability, the rotating stall mode or the surge mode, appears under the given conditions, while it is a matter of the compressor stability criterion to determine when compressor instability occurs (2,3). According to this concept the detrimental effect of rotating stall on the compressor performance i.e., pressure ratio and mass flow, may or may not cause the compression system stability criterion to be violated and thus initiate surge. Therefore, detailed knowledge of what happens in the rotating stall operation of a compressor seems to be of paramount importance to be able to understand and eventually influence the position of the stall limit line and the surge line.

In centrifugal compressor stalling it is a priori not known which of the two elements of a single stage centrifugal compressor, the impeller or the diffuser, causes the stalling of the stage. While stall criteria for vaneless diffusers are reported in the literature (4,5,6) and the diffuser stall phenomena are studied experimentally (7,8,9) no stall criterion for the impeller is known the authors which correlates well with experimental data. A stall model for axial compressors exists which is able to predict several features of axial compressor stall (10) whereas it appears to be much more difficult to formulate an equivalent stall model for the centrifugal impeller.

Earlier work reported about the same set up as was used in this investigation suggested that the impeller is the element that causes the stall of the stage at the speeds considered (11). Therefore, this work focusses more on impeller flow than on diffuser flow in order to get more detailed information about the flow through the impeller in rotating stall conditions.

EXPERIMENTAL FACILITIES

In this investigation a single stage centrifugal compressor with a vaneless diffuser was used. The aerodynamical and geometrical parameters of the tested compressor are listed in Table 1. The compressor map is shown in Fig. 1, where the total-to-total pressur ratio π_{tot} is plotted versus corrected mass flow and lines of equal isentropic efficiency η_{is} are given. The stall line was measured up to a speed of 18 000 rpm whereas the surge line was measured only up to 14 000 rpm because the operation of the compressor to the left of the stall line appeared to be too dangerous for the blading in the higher speed range. The surge line was found when the pressure in the suction chamber started to be unsteady, while the stall line was determined from inspection of an unsteady pressure signal

inlet diameter ratio	$d_{1,a}/d_2$	= 0.7
hub to tip ratio	$d_{1,i}/d_2$	= 0.225
exit width ratio	b_2/d_2	= 0.065
inlet blade angle	$\beta_{1,a}$	= 27°
exit blade angle	β_2	= 90°
diffuser radius ratio	d_3/d_2	= 2
number of blades (14 splitter blades)		28
diffuser area	$\pi \cdot d \cdot b$	= const.
circumferential Mach number	Mu	= 0.86

Table 1: Geometrical and Aerodynamical Parameters of the Tested Compressor

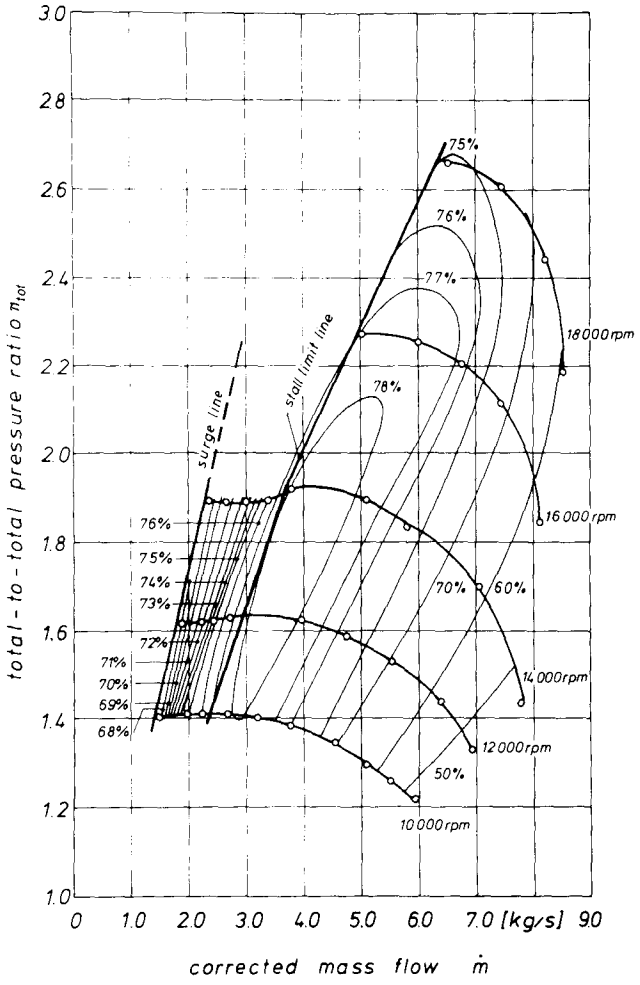

Fig. 1 Performance Map of Test Compressor

picked up at the compressor shroud line. In the fairly wide range between stall line and surge line a stable operation was possible while the internal flow of the compressor exhibited features of rotating stall. The stalled flow resulted in a drop

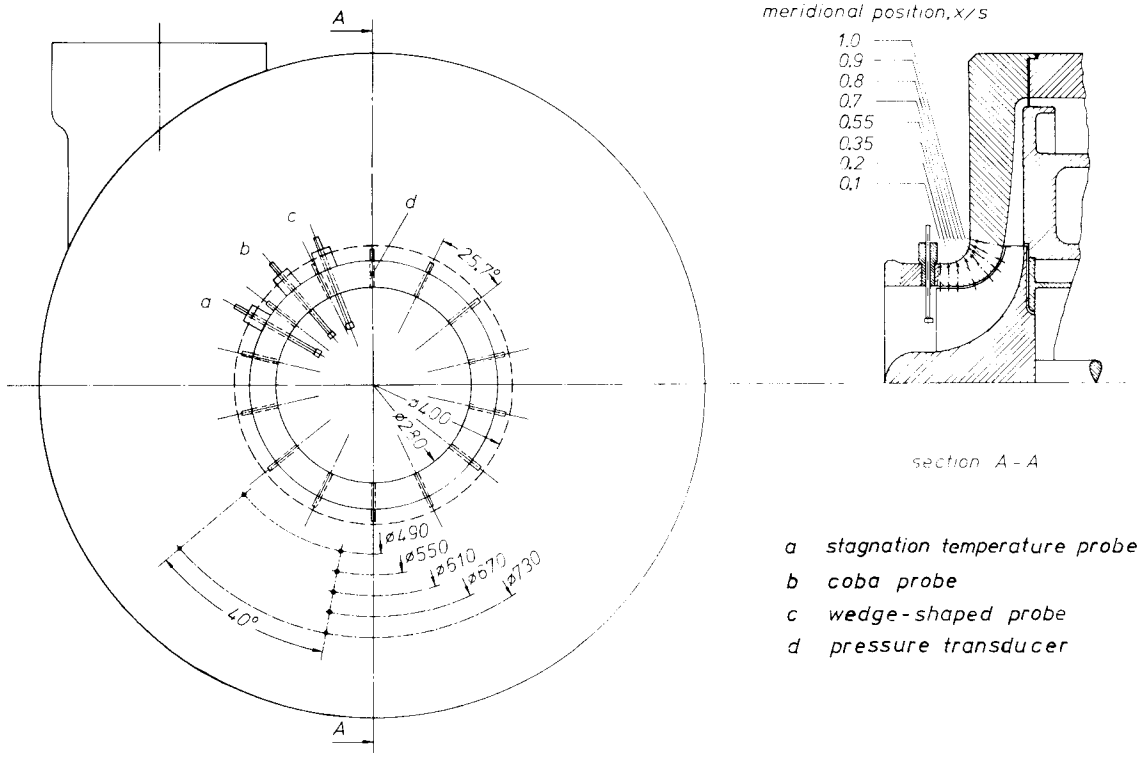

Fig. 2 Sketch of Test Compressor with Measuring Positions of Probes and Transducers

in pressure ratio and efficiency but did not violate the compression system stability criterion. Obviously, this was only violated after considerable further reduction of flow rate.

Steady and unsteady measurements were taken at the 12 000 rpm and 14 000 rpm speed lines. To investigate the approaching flow conditions three probes were traversed radially along the blade hight. A wedge-shaped probe was used to measure the static pressure and stagnation pressure, a cobra-probe to measure the flow angle and a third probe was used to measure stagnation temperature. Semiconductor pressure transducers were installed at the shroud line of the compressor to measure instantaneous static pressures. Two different arrangements of the pressure transducers were used in the tests. In the first arrangement 8 pressure transducers were positioned along the shroud line in such a fashion that a blade passed under all transducers simultaneously. Two transducers ahead of the impeller and three transducers in the diffuser were also included. In the other arrangement 14 transducers were installed along the circumference of the impeller shroud line. Fig. 2 gives a sketch of the test compressor and the measuring positions. The analysis of the measurements with the latter configuration is not included in this paper.

DISCUSSION OF RESULTS

Profiles of impeller inlet velocities and temperature

A typical result of the probe measurements 10 mm ahead of the impeller leading edge is plotted in Fig. 3. The axial and the circumferential velocities c_z and c_u are given in a normalized fashion. The axial velocity was normalized with a mean inlet velocity $\overline{c_z}$ at inlet chamber conditions for pressure and temperature and the circumferential velocity was normalized using the blade velocity at the outer diameter of the inlet plane, u_{1a}. The difference in stagnation temperature between the suction chamber temperature T_c and the inlet plane temperature T is also given in Fig. 3. For comparison, an axial velocity profile is included for an operating point, that did not exhibit rotating stall, indicated by the dashed line.

The results presented in Fig. 3 were obtained from the measurements at 14 000 rpm. The operating points were the one closest to the surge line and the one at 5.1 kg/s of mass flow rate which was to the right of the stall line. The picture given is representative for all results obtained at different operating points along the 12 000 rpm

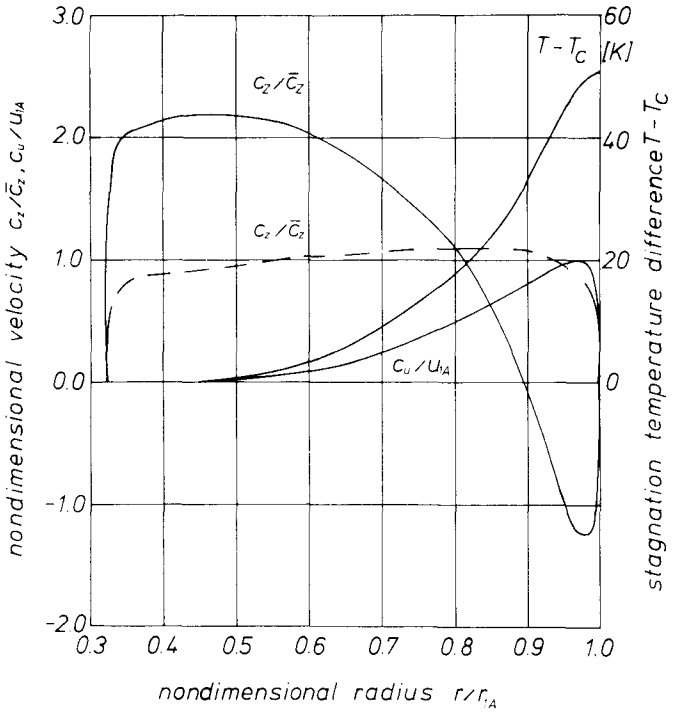

Fig. 3 Inlet Velocity and Temperature Profiles
---- $\dot{m}$ = 5.11 kg/s
——— $\dot{m}$ = 2.34 kg/s
n = 14,000 rpm

and the 14 000 rpm speed line in the range between the stall line and the surge line. Two interesting features are predominant. One can see a zone of reverse flow at the outer radius of the inlet annulus of a fairly large extend, and the magnitude of the back flow velocity is exceeding the mean axial velocity. At the smaller radii the positive axial velocity exceeds even twice the value of the mean velocity since here the net through flow and the reverse flow have to be fed into the impeller. The reverse mass flow amounted to up to 14 % of the net through flow. This picture is obviously characteristic for the stalled flow condition because a comparison with the unstalled flow velocity profile shows that in the latter case the axial velocity profile is fairly flat. The increase in axial velocity with radius is a consequence of the upstream effect of the impeller and agrees with calculations of the meridional velocity field.

A strong circumferential velocity component is also present in the approaching flow that is introduced through the reverse flow. It is of the same magnitude as the circumferential blade velocity in the outer radii and decays smoothly towards the core flow. It extends over the zone of reverse flow most likely because of mixing effects.

The reverse flow leaving the impeller is at a higher enthalpy level than the approaching flow due to energy transfer in the wheel. This is born out by the stagnation temperature distribution which reaches a maximum close to the outer radius of the inlet annulus. A considerable temperature rise of up to 50 K is observed. It decays very gradually and a noticeable temperature rise is found extending far into the core flow. This is also attributed to the mixing effects that take place in the volume upstream of the impeller where the high temperature swirling back flow mixes with the approaching cold axial flow. The combined effect of high axial flow and the peripheral velocity component in the core of the flow is to unload the leading edge of the impeller. This is demonstrated in Fig. 4, where the difference between the relative flow angle in the measuring plane and the blade leading edge angle at the particular radius is plotted. This corresponds to the incidence angle in case of the core flow zone, but in the reverse flow zone it indicates the flow direction relativ to the blades. Fig. 4 shows that throttling increases the incidence angle as long as no stall occurs. In stalled flow incidence is low in the core flow but in the reverse flow zone the plotted angle difference is different from 180 degrees, which means that the outflow is not parallel to the blades.

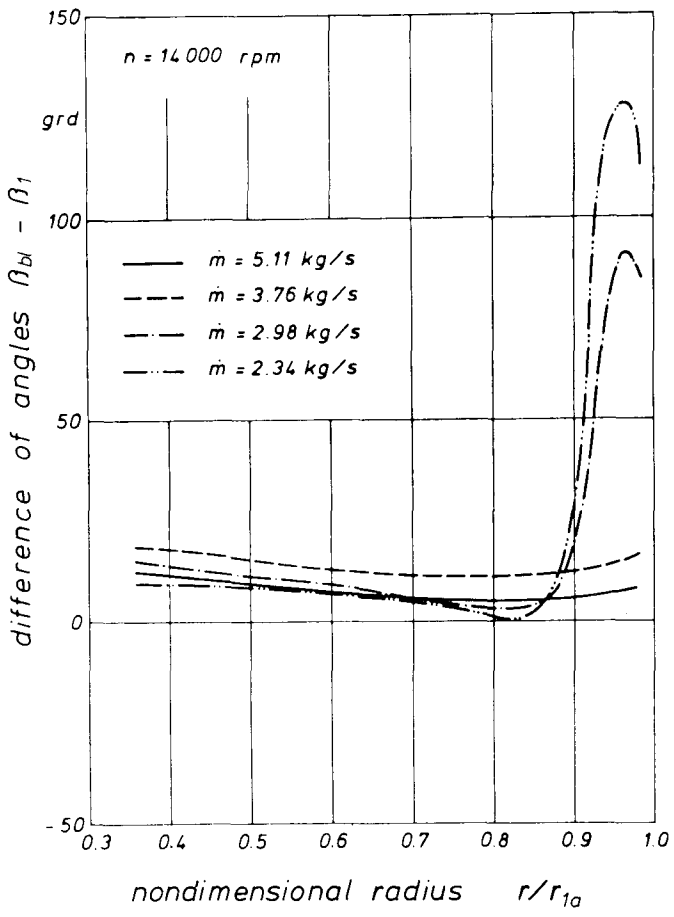

Fig. 4 Angle Difference $\beta_{b1} - \beta_1$ at Impeller Inlet

The question arises how the unsteady flow in the measuring plane effects the readings of stationary probes. Since unsteady probes have not been used in the inlet plane to attempt a measurement of the true, unsteady velocity field one only has the chance to judge the accuracy of the measurement by comparison of global values. The mass flow rate as measured with a conventional nozzle could be compared with the result that was obtained from an integration of the mass flow in the measuring plane. The readings of all three probes were introduced into the integration and axial symmetry was assumed. The two values differed by no more than 3 % and this was considered sufficiently accurate. Thus it is believed that the readings from the stationary probes give reasonably averaged values in an unsteady flow.

The drop of the pressure ratio and thus the degradation of efficiency with the beginning of rotating stall is partly due to the distorted inlet flow profile. Further reasons are seen in a possible reduction of efficiency of the energy transfer in the impeller and static pressure recovery in the diffuser when operating in stalled flow. The effect of the reverse flow is to introduce swirl and a temperature rise into the inlet velocity profile. The swirl reduces the wheel's potential to transfer energy to the flow. The elevated temperature moves the starting point of the compression process to higher enthalpy but at essentially the same pressure, thus giving a rise in entropy. In this way temperature rise and inlet swirl combine to lower the overall compressor efficiency.

Unsteady pressure signals

Rotating stall: Unsteady pressure signals were recorded on a magnetic tape with 14 channels for later analysis and evaluation. So far only frequency analyses have been performed but it is planned to perform an analysis in the time domain by which the shroud pressure field can be obtained in the stalled and unstalled moments during a revolution.

The unsteady recordings where taken at 12,000 rpm and 14,000 rpm but here only the results at 14,000 rpm are reported. Fig. 5 gives an impression of the nature of the pressure signals ahead of the impeller, in the impeller and in the diffuser for three mass flow rates on the 14,000 rpm speed line. The amplification factors are different for the 9 transducers but were kept constant for the three mass flow rates. For $\dot{m}$ = 5.10 kg/s the pressure signals exhibit the blade passing frequency as the dominating component whereas at $\dot{m}$ = 3.35 kg/s a low frequency fluctuation appears with a very large amplitude throughout the entire compressor. From the compressor map it is seen that this operating point is just to

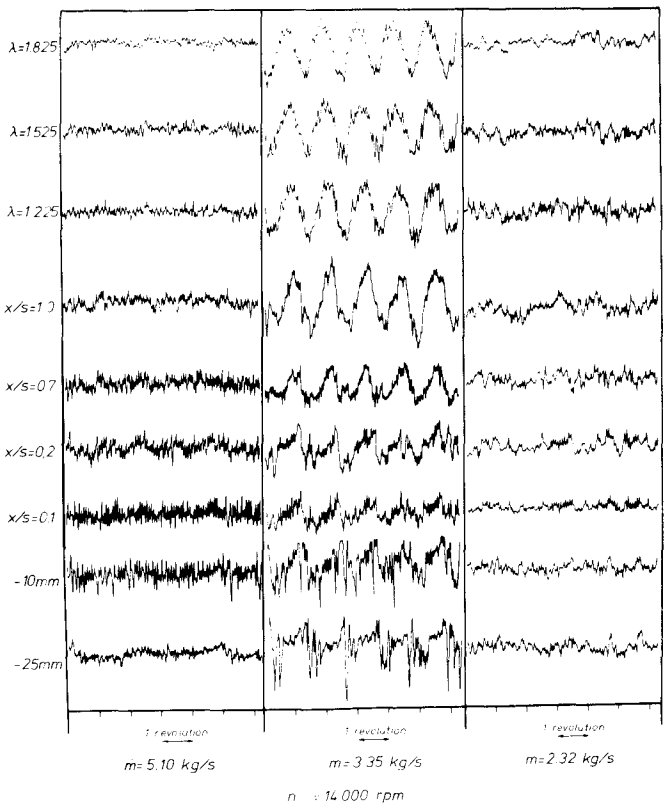

Fig. 5 Comparison of Pressure Signals with and without Stall

the left of the stall line. Further reduction of mass flow changes this picture again and at the operating point closest to the surge line, at 2.34 kg/s, the low frequency fluctuation disappeared again. However, pressure fluctuations in this case are still larger than it is the case for $\dot{m}$ = 5.10 kg/s and other frequencies besides the blade passing frequency are present in the pressure signals. While Fig. 5 shows the compressor stall in a qualitative fashion Fig. 6 gives the frequency spectra at 14,000 rpm for various mass flow rates between the unthrottled condition and the surge line.

A vibration peak at 100 Hz appears strongly in all the spectra. But it's magnitude is independent of mass flow rate and also independent of compressor speed, as was observed in the pressure spectra taken at 12,000 rpm. Therefore it is identified as the second harmonic of the power frequency and is not a physical characteristic of the flow. The reason for the strong appearance of the power frequency and it's harmonics is seen in the very long cables connecting the transducers and the recorder.

The frequency of rotation is 233 for a corrected speed of 14,000 rpm and accordingly a vibration peak is found at 237 Hz. The difference of 4 Hz is a result of the difference between corrected speed and actual speed. This peak appears most clearly

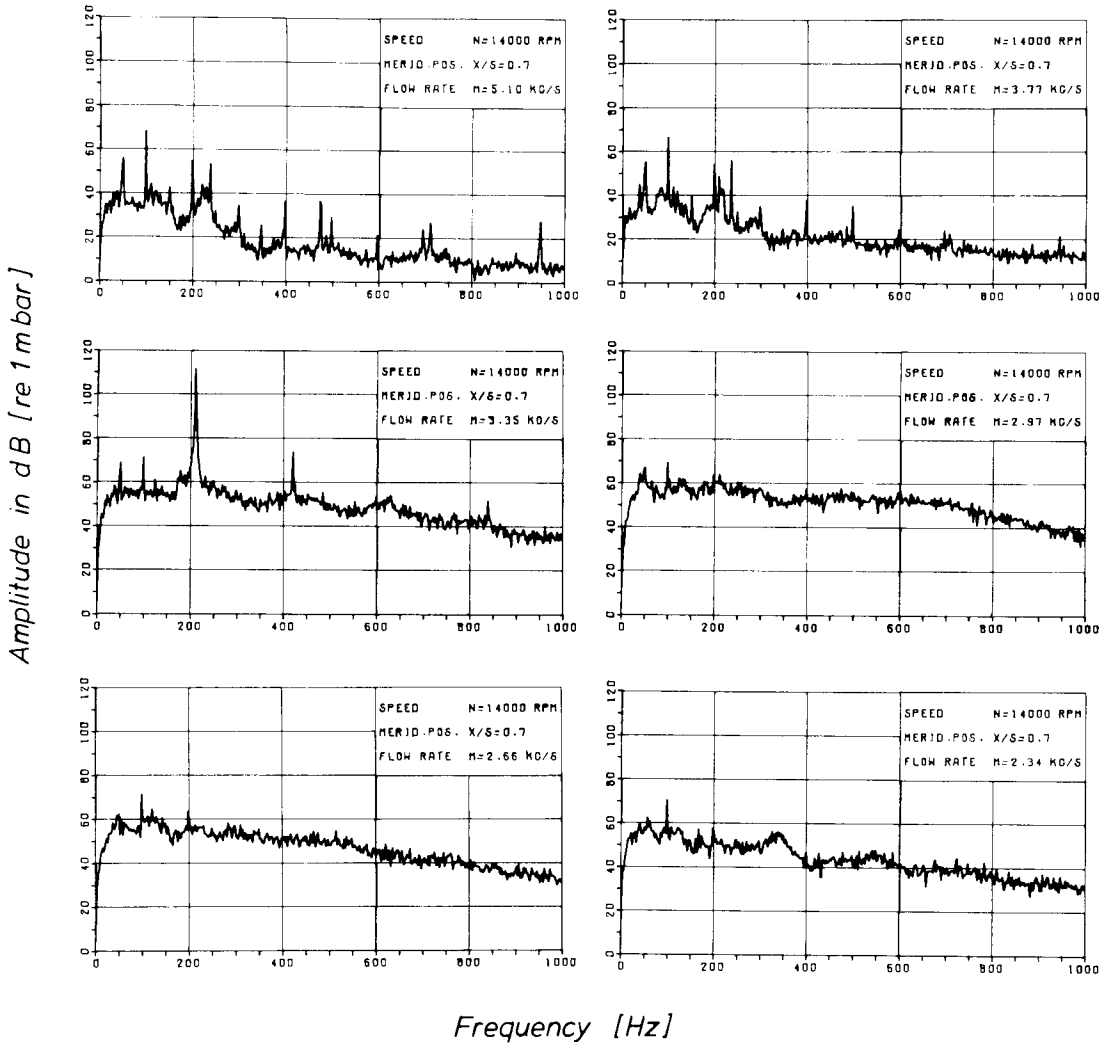

Fig. 6 Shroud Pressure Spectra at 14,000 rpm

in the spectra of the unstalled flow conditions. At a mass flow rate of 3.35 kg/s the picture changes completely and a peak of the stall frequency rises out of a fairly high background level. This stall frequency is at 211 Hz and can be clearly differentiated from the power line frequency as well as the frequency of rotation. This peak disappears if the mass flow is throttled further and though the mass flow rate is throttled almost to the surge line no stall frequency can be found.

Looking at the background level at frequencies above about 250 Hz it is fairly low in the spectra taken at 5.1 kg/s and 3.77 kg/s, having a value of about 20 dB. With the stalled flow this level rises up to about 50 dB, in the case of a distinct stall frequency at 3.35 kg/s as well as in the other stall conditions.

The impression is that only at a flow rate of 3.35 kg/s stall cells with a distinct frequency develop while with further flow reduction no coherent stall pattern is maintained. To have a closer look at this stall frequency spectral analyses were carried out for all meridionally spaced transducers at this flow rate and the amplitude of the stall frequency, plotted vs. the meridional path, is shown in Fig. 7. The stall amplitude is

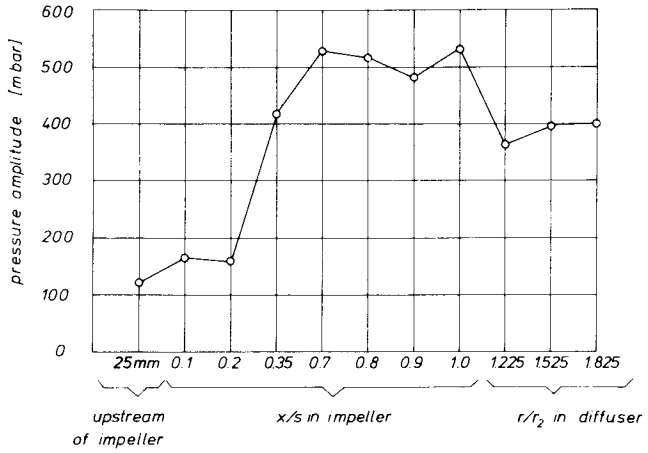

Fig. 7 Stall Frequency Amplitude
n = 14,000 rpm, $\dot{m}$ = 3.35 kg/s

growing slightly from the inlet duct to the inducer part of the impeller but large amplitudes are found in the radial part. Here the stall amplitude is almost constant over a large portion of the impeller length. In the diffuser the stall amplitude is lower than in the impeller but takes slightly larger values at the outer radii.

From Fig. 7 ist is concluded that the stall phenomena at 14 000 rpm and at 3.35 kg/s is introduced by the wheel and not by the diffuser. An origin inside the impeller cannot be clearly determined. A better understanding of the flow in this region is expected from detailed investigations of the pressure signals in the time domain.

The number of stall cells can be determined from the peripherally spaced transducers. From two transducers being displaced by an angle φ_g the number of cells m can be calculated by

$$m = \frac{\Delta\varphi}{\varphi_g} + \frac{2\pi k}{\varphi_g} \quad , \quad k = 0, 1, 2, \ldots \qquad (1)$$

with $\Delta\varphi$ being the angular difference of the two pressure signals. Assuming that the stall pattern propagates in the same direction as the impeller in the absolute frame of reference the value of $\Delta\varphi$ is between 0 and 2π. The factor k introduces an ambiguity into the determination of the number of cells, since it is not known how many cells lie completely between the transducer positions. Thus one wants to choose a small angle φ_g such that only k = 0 applies and already k = 1 gives unduely large value for m. On the other hand, choosing φ_g too small the inacurracy in the determination of $\Delta\varphi$ becomes large. Here $\varphi_g = 40^\circ$ seemed to be a good compromise.

In Fig. 8 two pressure signals from the diffuser are used to determine the number of stall cells. Averaging over 4 cycles of the stall frequency a phase angle difference of about 80° is obtained. This gives a number of m = 2 stall cells according to equation (1) if k = 0 is assumed. Using k = 1 would yield a value of m = 11 stall cells which is considered unlikely. Two stall cells and a stall frequency of 211 Hz result in a circumferential speed of the stall pattern of about 44 % of impeller speed. This value is somewhat higher than comparable values reported in (9).

Surge

Unsteady measurements of the pressures in the diffuser and the volumes and ducts upstream and downstream of the compressor were also taken during surge. The results of these experiments are not reported here in detail but an interesting feature of the surge behavior of the compressor shall be presented because it shows some similarity with the steady measurements during rotating stall. To visualize the flow direction during the surge cycle a wire with small, movable aluminium struts was mounted in the inlet duct of the compressor 40 mm ahead of the impeller. The position of these struts was recorded on a high speed film. Fig. 9 gives a picture of the inlet duct, the wire carrying the struts and the hole where the camera was mounted. Using a trigger on the film it was possible to synchronize the pictures on the film with the recorded pressure fluc-

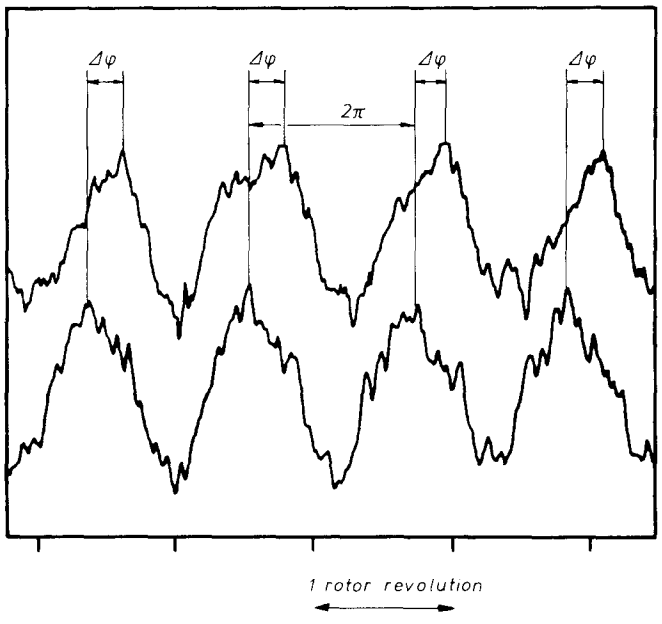

Fig. 8 Diffuser Static Pressure during Rotating Stall
λ = 1.825, n = 14,000 rpm
$\dot{m}$ = 3.35 kg/s, $\varphi_g = 40^\circ$

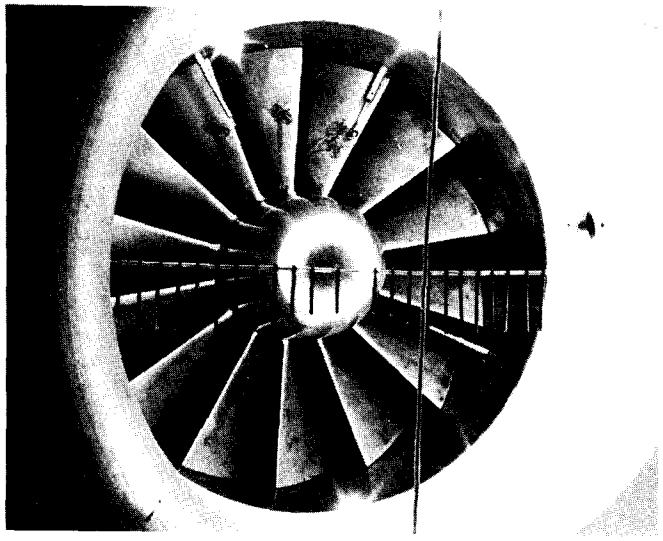

Fig. 9 View of Impeller Inlet

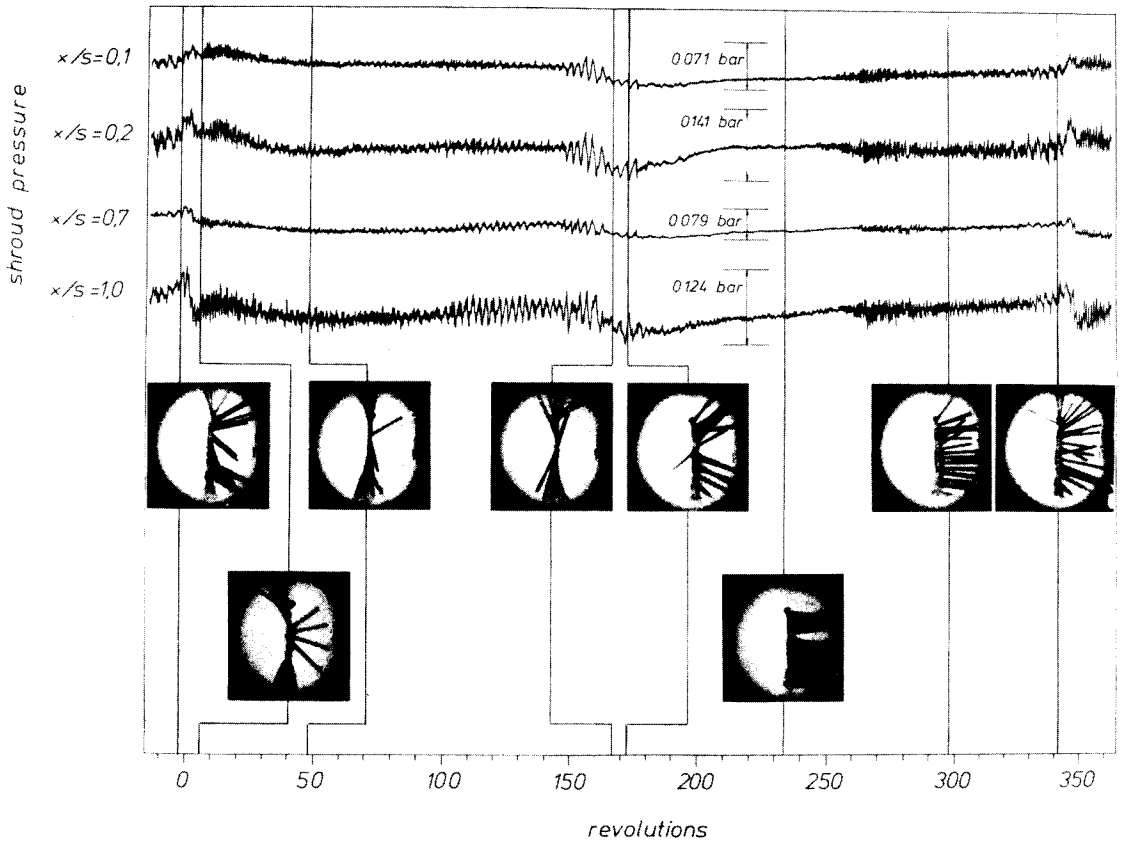

Fig. 10 Shroud Pressure and Inlet Flow Visualization during one Surge Cycle
n = 14,000 rpm

tuations. In Fig. 10 one complete surge cycle with the corresponding pressure signals at four positions at the shroud line is given together with pictures that show the flow direction in the individual phases of the surge cycle. The time is given in rotor revolutions. Counting of revolutions has started in the moment that is believed to be the inception of surge. The first picture shows the inlet flow just before surge inception where already several struts close to walls point into the circumferential direction. During the first half of the cycle the flow in the inlet duct is almost completely rotational and a component in the axial direction neither positive nor negative can be clearly identified. After about 160 revolutions the flow turns back into the axial direction with the transition taking not more than 5 rotor revolutions. Initially in the second part of the surge cycle the inlet flow is completely axial but a little later it can be observed that the struts close to the wall turn to the circumferential direction again. The static pressure signals have a high degree of fluctuation in the first part of the cycle as well as in the time shortly before surge inception. During the phase when the through flow is high fluctuations are very small. Obviously the impeller operates in a rotating stall mode before surge is initiated but over the complete surge cycle no back flow of any importance is present.

The position of the struts agree with the measurements shown in Fig. 3 but the pattern of swirl flow in the inlet duct is not only found during the rotating stall mode but also during the break down of the through flow that goes along with the initiation of surge.

SUMMARY

The steady measurements of the inlet flow profile of a centrifugal compressor revealed that a zone of reverse flow with a high circumferential velocity component was present in the inlet duct when the compressor operated in the rotating stall mode. The reverse flow mixed with the approaching flow and caused a swirl component and a higher temperature over almost the entire blade hight. It is believed that the deterioration of the inlet flow profile contibutes to the deterioration of efficiency when the compressor operates in rotating stall.

Unsteady pressure measurements showed that at the 14 000 rpm speed line a distinct stall pattern with two stall cells and a stall frequency of 211 Hz was only found over a small range of mass flow rate at about 3.35 kg/s. Further throttling completely changed the stalled flow such that

.o stall frequency or stall cells could be found. From the development of the stall frequency amplitudes along the shroud line of the compressor it is concluded that the stall is caused in the impeller.

Unsteady measurements during surge and the flow visualization by means of aluminium struts in the inlet duct showed a zone of reverse flow thus confirming the measurements in stationary rotating stall. Moreover, it was found that also during the break down of the through flow the flow pattern in the inlet duct was completely rotational and no back flow could be detected during the surge cycle.

ACKNOWLEDGEMENTS

Funds for this project were provided through a grant of the Deutsche Forschungsgemeinschaft.

REFERENCES

1 Greitzer, E.M., "Review-Axial Compressor Stall Phenomeny", Journal of Fluids Engineering, Vol. 102, June 1980

2 Stenning, A.H., "Rotating Stall and Surge", Fluid Dynamics of Turbomachinery, Chapter 15, ASME-Lecture Course, Iowa State University, 1973

3 Greitzer, E.M., "Surge and Rotating Stall in Axial Compressors", Part I and Part II, ASME-Paper No. 76-GT-9 and Paper No. 75-GT-10

4 Jansen, W., "Rotating Stall in Radial Vaneless Diffusers", Journal of Basic Engineering, Vol. 86, Dec. 1964

5 Senoo, Y., Kinoshita, Y., "Limits of Rotating Stall and Stall in Vaneless Diffusers of Centrifugal Compressors", ASME-Paper No. 79-GT-19

6 Abdelhamid, A.N., "Analysis of Rotating Stall in Vaneless Diffusers of Centrifugal Compressors", ASME-Paper No. 80-GT-184

7 Mizuki, S., Ariga, I., Kawashina, Y., "Investigation Concerning Rotating Stall and Surge Phenomena within Centrifugal Compressor Channels", ASME-Paper No. 78-GT-9

8 Abdelhamid, A.N., Calwill, W.H., Barrows, J.F., "Experimental Investigation of Unsteady Phenomena in Vaneless Radial Diffusers", ASME-Paper No. 78-GT-23

9 Abdelhamid, A.N., Bertrand, J., "Distinction Between Two Types of Self Excited Gas Oszillations in Vaneless Radial Diffusers", ASME-Paper No. 79-GT-58

10 Takata, H., Nagano, S., "Nonlinear Analysis of Rotating Stall", ASME-Paper No. 72-GT-3

11 Bammert, K., Rautenberg, M., "An Analysis of the Non-Steady and Non-Stable Flow Mechanisms in a Radial Compressor Impeller", ASME-Paper No. 77-WA/GT-4